Temporal asymmetry of fluctuations in nonequilibrium steady states: links with correlation functions and nonlinear response

Carlo Paneni*, Debra J. Searles*, Lamberto Rondoni**

** Nanoscale Science and Technology Centre, School of Biomolecular and Physical Sciences, Griffith University, Brisbane, Qld 4111, Australia (cpaneni@gmail.com, D.Bernhardt@griffith.edu.au)*

*** Dipartimento di Matematica and INFM, Politenico di Torino, Corso Duca degli Abruzzi 24, 10129 Torino, Italy (lamberto.rondoni@polito.it)*

February 7, 2008

Abstract

The presence of temporal asymmetries in fluctuation paths of nonequilibrium systems has recently been confirmed numerically in nonequilibrium molecular dynamics simulations of particular deterministic systems. Here we show that this is a common feature of homogeneously driven and thermostatted, reversible, deterministic, chaotic, nonequilibrium systems of interacting particles. This is done by expressing fluctuation paths as correlation functions. The theoretical arguments look rather general and we expect them to easily extend to other forms of driving and thermostats. The emergence of asymmetry is also justified using the transient time correlation function expression of nonlinear response theory. Numerical simulations are used to verify our arguments.

1 Introduction

A key issue in the study of nonequilibrium systems is the emergence of thermodynamic irreversibility from reversible equations of motion. Related to this issue is the question of the occurrence of temporally asymmetric behavior in exceptional fluctuations in nonequilibrium systems. Recently it has been shown that the usual stochastic models for nonequilibrium thermodynamic systems, such as Langevin dynamics, indicate a break of symmetry in fluctuations of thermodynamic properties in nonequilibrium states[1,2], and those studies have inspired the work presented in this paper. The theories extend the Onsager-Machlup fluctuation theory[3] to the nonequilibrium and non-linear domain. Concisely, they lead to the introduction of a term in the "adjoint" hydrodynamic equations, the equations describing the fluctuations away from the nonequilibrium steady states, that has no counterpart in the usual hydrodynamic equation. That is, for a system where the equations describing the relaxation toward the nonequilibrium steady states are given by

$$\partial_t \rho = \mathcal{D}(\rho), \tag{1}$$

the "adjoint" hydrodynamic equations are given by,

$$\partial_t \rho = \mathcal{D}^*(\rho) \tag{2}$$

where $\mathcal{D}^*$ is, in general, non-local and different from $-\mathcal{D}$. The theories apply to stochastic lattice gases that admit a hydrodynamic description, but are supposed to hold more generally, under some assumptions[1,2], if the mesoscopic evolution is given by a Markov process. An alternative approach has been to directly monitor the response and relaxation of a system due to a change in the applied field, and a recent investigation in that regard was made by Gaspard[4].

Temporal asymmetries have also been experimentally observed on stochastically perturbed electrical circuits analogous to a form of Brownian motion in a force field with weak white noise[5,6]. It is therefore clear that stochastic models show asymmetric behavior in the fluctuations of their properties, and the following question arises: would asymmetry in fluctuations of dynamical properties occur in the usual molecular-level models of thermodynamic systems, which are reversible and deterministic? In the studies on the perturbed electrical circuits, the symmetry of typical large fluctuations in steady state systems was examined. Previously[7,8] we have used a similar approach to verify that reversible, deterministic systems exhibit temporal asymmetries for two reversible and deterministic nonequilibrium simulated systems. We therefore confirmed that the asymmetry is not an artifact of the stochastic representation. This was also observed in reference[9,10].

In our earlier work on homogeneous Couette flow, it was necessary to use time dependent periodic boundary conditions. This introduces periodic fluctuations to the properties, and their influence needs to be carefully removed[7]. Furthermore the geometry of this system might be thought to introduce artificial asymmetry. For these reasons we decided to consider a somewhat simpler system: that which involves the flow of colored particles due to a color field.

In previous work, we limited ourselves to numerical observation of asymmetry in carefully defined "typical" fluctuation paths (FPs) for a number of observables of N-particle systems, but we gave no theoretical analysis. Here we introduce a new definition of FPs that allows us to confirm the ubiquity of the results obtained. Using this we justify the presence of asymmetry by reformulating the FPs as correlation functions and also using nonlinear response theory: we therefore give a first theoretical explanation of this phenomenon for deterministic and reversible systems. To substantiate our analysis, we use nonequilibrium molecular dynamics simulations.

As well as considering temporal asymmetries in typical FPs, as was done previously[7,8,9], in this work we also look at asymmetry in general time correlation functions, *i.e.*we examine if Onsager type relations, $\langle A(t)B(t-s)\rangle - \langle A(t)B(t+s)\rangle$, become nonzero out of equilibrium for these systems[11,12,13,14,15]. We provide some general arguments and present numerical results.

2 Simulated system and definition of fluctuation paths

2.1 System

The purpose of the paper is to understand how asymmetric fluctuations can arise in homogeneously driven and thermostatted nonequilibrium systems composed of interacting particles whose positions evolve according to deterministic, reversible dynamics. The theoretical treatment applies to this class of nonequilibrium particle systems, and we expect it to extend to more general nonequilbrium systems. For the sake of illustration, in the numerical work we choose a many-particle system where the particles interact via the Weeks-Chandler-Andersen potential (WCA)[16]:

$$V^{WCA}(r_{ij}) = \begin{cases} V^{LJ}(r_{ij}) + \varepsilon & if \quad r_{ij} < r_{\min} \\ 0 & if \quad r_{ij} \geq r_{\min} \end{cases} \tag{3}$$

where $V^{LJ}(r_{ij})$ is the two-body Lennard-Jones potential :

$$V^{LJ}(r_{ij}) = \sum_i \sum_{i>j} 4\,\varepsilon \left(\left(\frac{\sigma}{r_{ij}} \right)^{12} - \left(\frac{\sigma}{r_{ij}} \right)^{6} \right) \tag{4}$$

ε and σ are specified parameters; r_{ij} is the separation between each pair; $r_{min} = 2^{\frac{1}{6}}\sigma$ and $\varepsilon = -V^{LJ}(r_{min})$. The WCA potential is therefore the Lennard-Jones potential truncated at the position of minimum potential energy $\left(r_{ij} = 2^{\frac{1}{6}}\sigma\right)$ and then shifted up so that the potential and its derivative are zero at the cut-off radius[17]. In order to efficiently represent a microscopic part of a macroscopic system without incurring large boundary effects, we use periodic boundary conditions. Since our attention is towards phenomena that take place in a nonequilibrium steady state, we chose a simple and well known system: that in which color diffusion occurs. This models the flow of particles of opposite "color" charge. That is, they experience a force due to an external field that depends on their color, but the pair interaction potential is independent of their color. The field does work on the system so, to prevent it from heating and enable a steady state to be reached, a reversible thermostat is applied[18]. The system is similar to a thermostatted system of charged particles to which a field is applied, except that the particles are not influenced by the charges on other particles. The system's unthermostatted dynamics are driven by the color Hamiltonian[18,20]:

$$H = H_0 - \sum_{i=1}^{N} c_i q_{xi} F_c \tag{5}$$

where q_{xi} is the x-direction component of the laboratory coordinates particle i; H_0 is the unperturbed Hamiltonian or internal energy of the system; c_i is the color charge of particle i (we select an equal number of positive and negative color charges and $c_i = (-1)^i$) ; and F_c is the color field, which is applied in the x-direction in this case. The equations of motion that drive the trajectories of the particles are the following:

$$\dot{\mathbf{q}}_i = \frac{\mathbf{p}_i}{m_i} \tag{6}$$

$$\dot{\mathbf{p}}_i = \mathbf{F}_i + c_i F_c \hat{\mathbf{n}}_x - \zeta(\mathbf{p}_i - \mathbf{P}) \tag{7}$$

$$\zeta = \frac{\sum(\mathbf{p}_i - \mathbf{P}) \cdot (\mathbf{F}_i + c_i F_c \mathbf{i})}{\sum(\mathbf{p}_i - \mathbf{P}) \cdot \mathbf{p}_i} \tag{8}$$

where $\mathbf{q}_i$ is the laboratory coordinate of particle i; $\mathbf{p}_i$ its peculiar momenta; $\mathbf{F}_i$ is the force due to its interaction with other particles; and $\mathbf{P} = \frac{1}{N}\sum_{i=1}^{N} \mathbf{p_i}$ ensures that the total momentum stays fixed. ζ is the Gaussian thermostat multiplier, determined using Gauss's principle of least constraint, which keeps the kinetic temperature $\sum_{i=1}^{N} \frac{(\mathbf{p}_i - \mathbf{P})^2}{2m_i} = (dN - d - 1)k_B T/2$ fixed, where k_B is Boltzmann's constant and d is the number of Cartesian dimensions. This constraint ensures that the trajectories actually followed by our system are those which deviate as little as possible, in a least square sense, from the

unconstrained ones. In the simulations, we choose the total momentum to be zero initially, and from the equations of motion this means $\mathbf{P} = \mathbf{0}$ at all times. The adiabatic heating effect (*i.e.* the change in internal energy in the absence of the thermostat) or dissipation, can be expressed in terms of the product of the dissipative flux and the field:

$$\dot{H}_0^{ad} = -JF_cV = J_cF_cN \tag{9}$$

where J is the dissipative flux which is related to the color current $J_c = \frac{1}{N}\sum_{i=1}^{N} c_i\dot{q}_{xi} = -JV/N$. We note that p_{xi} includes a streaming contribution due to the flow of particles of each color. If a realistic thermostatting mechanism was desired, this would be problematic and this contribution should be subtracted. However it is not possible to know the real streaming component in this system *a priori* and, as discussed in Appendix A, there are issues in determining the correct nonlinear response expression in small systems when a instantaneous approximation to this contribution is made (as is common practice, see for example Chapter 6 of reference[18]). As the main objective of this paper is to identify asymmetry in a well defined, small, nonequilibrium system, and not in providing realistic thermostatting mechanism, we choose the model above. This will not alter our conclusions, and is a reasonable physical model at low fields.

The color diffusion equations of motion above are time reversal invariant under the time reversal mapping $i^{\mathcal{R}}$, which inverts the signs of the components of the molecular momenta,

$$i^{\mathcal{R}}\left(x_i, y_i, p_{xi}, p_{yi}\right) = \left(x_i, y_i, -p_{xi}, -p_{yi}\right). \tag{10}$$

That is:

$$i^{\mathcal{R}}S^t i^{\mathcal{R}} S^t \mathbf{\Gamma} = \mathbf{\Gamma} \tag{11}$$

where $S^t\mathbf{\Gamma}$ is the solution of Eqs.(6, 7, 8) with initial condition $\mathbf{\Gamma} \in \mathcal{M}$, where $\mathcal{M}$ is the phase space of the system.

We use Lennard-Jones reduced units throughout this paper[17].

2.2 Fluctuation Paths

Although our numerical results refer to the specific system discussed in Section 2.1, the theoretical arguments apply much more generally. Consider a dissipative system driven by a field, F_e, producing a dissipative flux, J. Figure 1 displays a sample of the values of the dissipative flux, J over a short period in a typical nonequilibrium system. Several signatures of irreversibility are clearly observable: the mean value of the dissipative flux is lower than zero; the probability of observing positive values

of J is smaller than that of observing negative values, and the distribution of values of J is skewed towards negative values. Fluctuation Relationships and Theorems[21,22] have been developed over the past 10 years that assist in explanation of these phenomena. Here we focus our attention on another signature of irreversibility: the temporal asymmetry in typical FPs. There are many ways of defining a FP. However, as discussed previously[7,8], provided the definition is precise and identifies symmetry at equilibrium, the most suitable definition will depend on the details of the investigation. In this paper we abandon the definition that has been considered in the past[7,8,9] and choose one that seems as intuitive, physically reasonable and computationally efficient, but has the advantage that it can be easily expressed in a correlation function formalism, as shown in Section 4.[23] In practice, we wish to compare the paths that take the instantaneous value of the observable away from its mean value with those that bring it towards this value: ultimately we want to see if the rise of a typical fluctuation is more or less steep than its decay back to the mean value. In our construction of the FP, we define a threshold T_{HR} (in the example of Figure 1 it is set equal to $|\mu - 1.5\sigma|$, where μ is the mean and σ is the standard deviation of the distribution of fluxes) and a time interval τ.[24] We consider the stationary points (maxima and minima) whose absolute value exceeds the selected threshold T_{HR}. For every such stationary point, we define t_{STAT} to be the time at which this stationary point is observed, and we consider the ordered set of values that the property assumes for the time interval τ before t_{STAT} and for the time interval τ after t_{STAT} (refer again to Figure 1). For every stationary point whose absolute value exceeds the selected threshold T_{HR}, the FP is the set of absolute values that the property under interest assumes in the time interval of width 2τ interval about the stationary point (refer to Figure 1). Of course the discrete nature of the simulated dynamics means that observation of points with $\dot{X} = 0$ is not possible in practice, so in the simulations we identify stationary points above the threshold using the condition that $t = t_{STAT}$ when $sign(X(S^{t+\Delta t}\mathbf{\Gamma}) - X(S^t\mathbf{\Gamma})) = sign(X(S^{t-\Delta t}\mathbf{\Gamma}) - X(S^t\mathbf{\Gamma}))$, where Δt is the timestep used in the simulation and $sign\left(X\left(\mathbf{\Gamma}\right)\right)$ is the sign of $X\left(\mathbf{\Gamma}\right)$.

Insert Figure 1 near here

More precisely, we define a FP as the series of values that the property assumes in an interval $[t_{STAT} - \tau; t_{STAT} + \tau;]$, multiplied by the sign of $X(t_{STAT})$. So, given an observable $X(t) \equiv X\left(S^t\mathbf{\Gamma}\right)$ with mean μ, we select the time width of interest, $\tau > 0$, and a positive threshold value $T_{HR} \neq \mu$, then, for every t_{STAT} (see Figure 1) such that $\left|X\left(t_{STAT}\right)\right| > T_{HR}$ and $\dot{X}\left(t_{STAT}\right) = 0$, we define the observable Y_t, for $t \in [-\tau, \tau]$ as: $Y_t = sign(X(t_{STAT}))X\left(t_{STAT} + t\right)$ for $t \in [-\tau, \tau]$. The time-ordered set of values Y_t, with $t \in [-\tau, 0]$ defines the path leading toward stationary point or the rise; the time-ordered set of values Y_t, with $t \in [0, \tau]$ defines the path leading away from the stationary point or the fall; the combination of the two sets defines the FPs. For every t_{STAT} such that

$|X(t_{STAT})| > T_{HR}$, $\dot{X}(t_{STAT}) = 0$ and $\ddot{X}(t_{STAT}) < 0$, we say the observable Y_t belongs to a "Peak"; while if $\ddot{X}(t_{STAT}) > 0$, we say it belongs to "Trough".

In order to identify the typical FP, we consider the average of all the FPs. Evaluating the average FP is computationally simpler than evaluating the most probable FP, as has been done in some previous studies[7,8]. In the thermodynamic limit (infinite N), if a single FP is expected, they will be identical. Even with a small number of particles (N=8), the most probable and average FPs have been observed to be very similar for these systems (see Fig 2 of [7]).

The fluctuation relations mentioned above show that, for an odd property, the probability of having values one side of zero will be greater than the other. Therefore at large fields, if the mean is large and positive, it will be by far more likely to find peaks above the threshold than troughs under the threshold (the opposite for mean below zero). For positive definite or negative definite properties, only one of the two will be possible, since the property can only be positive or can only be negative. If we set thresholds far from the mean (which we must, since we are interested in exceptional fluctuations) we will be unlikely to find peaks below $-T_{HR}$ or troughs above T_{HR}. Ultimately, the average FP so defined will turn out practically to coincide with the average of peak FPs (if the mean is above zero) or with the average of trough FPs (if the mean is below zero). Numerical results confirm this assertion.

To quantify the asymmetry, we define an asymmetry coefficient. Given any FP of time width τ and threshold T_{HR}, we define the measure of asymmetry δ_t for $t \in [0, +\tau]$ of the FP as:

$$\delta_t = Y_{-t} - Y_t \tag{12}$$

In order to identify the asymmetry arising in the FP, the average of δ_t over all the steady state fluctuation paths, $\langle \delta_t \rangle$, will be plotted for different values of $t \in [0, +\tau]$. Provided $\langle \delta_t \rangle$ is not zero for every t, the FP is asymmetric. However, if a null result is obtained we could not definitively rule out asymmetry, as it might be an artifact of the method adopted. We note that in our previous work the time integral of $\langle \delta_t \rangle$ was used to measure the asymmetry[7,8].

3 Correlation Functions and nonlinear response theory for determination of asymmetry

3.1 Correlation Functions

Using the definition above, we can show how the coefficient of asymmetry $\langle \delta_t \rangle$ can be expressed as a difference of cross correlation functions. Let $X(\mathbf{\Gamma})$ be the phase variable whose asymmetry is being

investigated. Let us consider the following functions $A(\mathbf{\Gamma})$ and $B(\mathbf{\Gamma})$:

$$A(\mathbf{\Gamma}) = X(\mathbf{\Gamma}) \tag{13}$$

$$B(\mathbf{\Gamma};\Delta t) = \begin{cases} 0 & if \quad |X(\mathbf{\Gamma})| < T_{HR} \quad or \quad sign(\Delta X(\mathbf{\Gamma},\Delta t)) \neq sign(\Delta X(\mathbf{\Gamma},-\Delta t)) \\ sign(X(\mathbf{\Gamma})) & if \quad |X(\mathbf{\Gamma})| > T_{HR} \quad and \quad sign(\Delta X(\mathbf{\Gamma},\Delta t)) = sign(\Delta X(\mathbf{\Gamma},-\Delta t)) \end{cases} \tag{14}$$

where $\Delta X(\mathbf{\Gamma},\Delta t) = X(S^{\Delta t}\mathbf{\Gamma}) - X(\mathbf{\Gamma})$ and Δt is the simulation timestep. An equivalent way of writing this is:

$$B(\mathbf{\Gamma};\Delta t) = sign(X(\mathbf{\Gamma}))\,\Theta(|X(\mathbf{\Gamma})| - T_{HR}) \mid sign(\Delta X(\mathbf{\Gamma},\Delta t)) + sign(\Delta X(\mathbf{\Gamma},-\Delta t)) \mid /2 \tag{15}$$

where $\Theta(r)$ is the Heaviside step function ($\Theta(r)$ =1 if $r > 0$ and $\Theta(r)$=0 otherwise). In the limit $\Delta t \to 0$, $B(\mathbf{\Gamma};\Delta t) \to B(\mathbf{\Gamma})$ and is therefore simply equal to +1 for stationary points Γ above T_{HR} ; it is equal to -1 for stationary points below $-T_{HR}$; and is it equal to 0 otherwise. We can therefore write Y_t as:

$$Y_t = X\left(S^t\mathbf{\Gamma}\right) B(\mathbf{\Gamma}) \tag{16}$$

with $t \in [-\tau, +\tau]$, and this describes a FP if $B(\mathbf{\Gamma}) \neq 0$, i.e. if Γ is a stationary point with $|X(\Gamma)| > T_{HR}$.

If we take the (conditional) ensemble average over all $\mathbf{\Gamma}$ for which $B(\mathbf{\Gamma}) \neq 0$, we obtain an average FP:

$$\langle Y_t \rangle_C = \frac{\langle A(S^t\mathbf{\Gamma})\,B(\mathbf{\Gamma})\rangle}{\langle |B(\mathbf{\Gamma})| \rangle} = \left\langle A\left(S^t\mathbf{\Gamma}\right) B(\mathbf{\Gamma})\right\rangle_C = \left\langle X\left(S^t\mathbf{\Gamma}\right) B(\mathbf{\Gamma})\right\rangle_C \tag{17}$$

where $\langle ... \rangle_C$ denotes a conditional average. Note that $\langle |B(\mathbf{\Gamma})| \rangle$ is the proportion of phase points that meet the selection criterion. It is necessary to take a conditional average here as we wish to obtain a result that is consistent with past numerical results for $\langle \delta_t \rangle$. In cases where very few peaks meet the selection criteria, the complete ensemble average would be a very small number. Using Eq (12) and the definition of $\langle \delta_t \rangle$, we can write:

$$\langle \delta_t \rangle = \left\langle X\left(S^{-t}\mathbf{\Gamma}\right) B(\mathbf{\Gamma})\right\rangle_C - \left\langle X\left(S^t\mathbf{\Gamma}\right) B(\mathbf{\Gamma})\right\rangle_C . \tag{18}$$

The dynamical properties we are interested in are either symmetric or antisymmetric under time reversal mapping: $X\left(i^{\mathcal{R}}\mathbf{\Gamma}\right) = p_X X(\mathbf{\Gamma})$, where $p_X = \pm 1$ is the parity of $X(\mathbf{\Gamma})$. We observe from Eq. (16) that Y_t is an even function when A and B are defined by Eqs (14, 13): that is $p_{AB} = 1$. This result is obtained by firstly noting that $A\left(i^{\mathcal{R}}\mathbf{\Gamma}\right) = p_X A(\mathbf{\Gamma})$. It is straightforward to see that

$\Theta\left(|X\left(\mathbf{\Gamma}\right)|-T_{HR}\right)$ and the delta function of the time derivative of X, $\delta\left(\dot{X}\left(\mathbf{\Gamma}\right)\right)$, do not change with time reversal symmetry, and that, $sign\left(X\left(\mathbf{\Gamma}\right)\right)$ has the same parity as $X\left(\mathbf{\Gamma}\right)$. Therefore the parity of B will be the same as that of $X\left(\mathbf{\Gamma}\right)$, and $p_{AB}=p_{A}p_{B}=p_{X}p_{X}=1$. We can also consider the behavior of the average FPs on reversal of the sign of F_e. We note that in the definition of Y_t, the value of $X(t_{STAT}-t)$ is multiplied by the sign of $X(t_{STAT})$ to ensure that FPs are always positive at the peak. This could destroy the smoothness of Y_t as a function of F_e at $F_e=0$ if the field changes the sign of $\langle X\rangle$ (*e.g.* if the dependence on F_e is linear) and therefore in analyzing the behavior of the FPs as a function of F_e we consider the paths defined without this change in sign ($i.e. sign(X(t_{STAT})Y_t)$. We note that there is no explicit dependence of A or B on the field, however the nonequilibrium distribution function will change, and therefore the ensemble average may change. Therefore, we introduce the symbol $\langle A\rangle_{F_e}$ to denote the phase space average computed with respect to the steady state distribution obtained with field F_e, and p_{A,F_e} for the parity of A with respect to the sign of F_e. We observe that if $\langle A\rangle_{F_e}=p_{A,F_e}\langle A\rangle_{-F_e}$ then $\langle sign(X(t_{STAT}))Y_t\rangle_{F_e}=p_{A,F_e}\langle sign(X(t_{STAT}))Y_t\rangle_{-F_e}$.

Now that we have the average FP expressed as a correlation function, we can use properties of correlation functions to infer some properties of the FP. Table 1 lists a number of properties of a correlation function $C(z,t)=\langle A(z+t)B(z)\rangle$. These were obtained by considering the symmetry of the functions on time-reversal and change of the sign of the field, and assuming that correlations decay in the all the systems considered. At equilibrium and in steady states, the value of $C(z,t)$ is independent of z, but not necessarily of t. Furthermore, at equilibrium the time-reversal invariance of the distribution function can be used to show that $C(z,0)=0$ if $p_{AB}=-1$, and $d(C(z,t))/dt|_{z,t=0}=0$ if $p_{AB}=1$.

Using the information in Table 1, firstly we note that the identification of asymmetry through examination of $\langle A(z-t)B(z)\rangle-\langle A(z+t)B(z)\rangle$ should be carried out with caution, as in the steady state, selection of some combinations of A and B will give a value of 0 for this difference. Another important deduction is that the selection of A and B given in equations (13) and (15) will result in $\langle\delta_t\rangle$ that becomes 0 in the linear regime if $p_{X,F_e}=1$. In contrast, if $p_{X,F_e}=-1$, the asymmetry might be linear in F_e. We find that for fixed threshold, our results are consistent with a F_e^2 dependence of $\langle\delta_t\rangle$ on F_e for the pressure and with a F_e dependence for the color current, in accord with this deduction. We also note that in the limit of long t, our measure of asymmetry will go to zero.

Another important observation can be made when considering steady states. We note that if there is any correlation between the functions A and B, then $(C(z,0)-\langle A\rangle\langle B\rangle)$ will be non-zero, but $(C(z,\infty)-\langle A\rangle\langle B\rangle)=0$. If correlation between A and B exists and the correlation time is finite, in general $\dot{C}(z,t)|_{z,t=0}\neq 0$, although this will not be the case if $\dot{A}|_{z,t=0}=0$ for all $B(z)\neq 0$ or if $A=B$,

$\dot{A} = B$, etc. Similarly, $\frac{d^2C(z,t)}{dt^2}|_{z,t=0}$, $\frac{d^3C(z,t)}{dt^3}|_{z,t=0}$, ... will be non-zero in general. However, we know that in the limit of large t, $C(z,t) = \langle A\rangle\langle B\rangle = C(z,-t)$ because we assumed decay of correlations. As demonstrated in Figure 2, these features and any non-zero value of an odd time-derivative of $C(z,t)$ at $t = 0$ indicate that asymmetry must exist. This is an important result as it means that it is not necessary to monitor the full FP, it is sufficient to know $C(t,0)$, $\dot{C}(z,t)|_{z,t=0}$, $\frac{d^3C(z,t)}{dt^3}|_{z,t=0}$ and $\langle A\rangle\langle B\rangle$. This is computationally much more straightforward, and in most cases the fact that $\dot{C}(z,t)|_{z,t=0}$ and $\frac{d^3C(z,t)}{dt^3}|_{z,t=0}$ are non-zero can be inferred from the facts that A and B are correlated and the correlation time is finite.

For example it would be expected that if A is the pressure (P) and B is the current (J_c) asymmetry would occur as $\langle\dot{P}(z,t)J_c(z)\rangle \neq 0$ when $t = 0$. As mentioned above, if $\frac{d^nC(z,t)}{dt^n}|_{z,t=0} = 0$ for all $n = 1,3,5,...$, this is insufficient to rule out asymmetry as it might be due to the definition of the FP, but if $\frac{d^nC(z,t)}{dt^n}|_{z,t=0} \neq 0$, for any $n = 1,3,5,...$, asymmetry is present.

Insert Figure 2 near here

For the correlation function developed to produce $\langle\delta_t\rangle$, (*i.e.*equations (13-14)), it can be seen that $\dot{A}|_{z,t=0} = 0$ for all $B(z) \neq 0$ since this is used as a selection criteria in conditional average. Therefore $\dot{C}(z,t)|_{z,t=0} = 0$ in this case, and the argument based on the first derivative in the previous paragraph cannot be used to predict asymmetry in the FPs. However, the third-derivative is not subject to such a condition, and would be expected to be non-zero at $t = 0$; so $\langle\delta_t\rangle$ would not vanish and asymmetry in the FPs would exist. This indicates that $\langle\delta_t\rangle \neq 0$ and asymmetry in the FPs exists.

The above arguments rest on the assumption that correlations decay in time, however the rate of decay is not specified and any decay rate will suffice. In contrast, in the following subsection integrals of the correlation functions appear, and then it will be required that these correlations decay sufficiently fast for the integrals to exist.

Insert Table 1 near here

3.2 Nonlinear response theory

Since we have expressed the asymmetry coefficient, $\langle\delta_t\rangle$, in terms of a ensemble average of a phase function, we can also apply nonlinear response theory to its analysis. The advantage of this approach, for the purposes of this work, is that it allows a nonequilibrium, time-dependent phase function to be expressed in terms of an ensemble average over equilibrium initial states.

Using nonlinear response theory, the transient time correlation function (TTCF) provides the time-dependence of a phase function in a nonequilibrium steady states far from equilibrium[18] . In the long

time limit, for a system that reaches a steady state, it can be considered to be a generalization of the Green-Kubo relations[25] to states far from equilibrium as it provides an expression for the flux, from which the non-linear transport coefficients can be determined. It allows us to express the average value of a function $\langle A\left(S^{z}\mathbf{\Gamma}\right)\rangle_{eq}$ at time z after equilibrium in terms of its value at equilibrium $\langle A\left(\mathbf{\Gamma}\right)\rangle_{eq}$ and an integral of a time correlation function, which in homogeneously driven and thermostatted systems (see Appendix A) is given by:

$$\langle A(S^{z}\mathbf{\Gamma})\rangle_{eq}=\langle A(\mathbf{\Gamma})\rangle_{eq}-\beta VF_{e}\int_{0}^{z}\langle J\left(\mathbf{\Gamma}\right)\Delta A\left(S^{u}\mathbf{\Gamma}\right)\rangle_{eq}du \tag{19}$$

where $J(\mathbf{\Gamma})$ is the dissipative flux and $\Delta A(S^{u}\mathbf{\Gamma})=A(S^{u}\mathbf{\Gamma})-\langle A\rangle_{eq}$. The dynamics S^{u} is generated using the nonequilibrium (thermostatted) equations of motion, but the ensemble averages use the equilibrium distribution. This can directly be extended to express the product of two functions $A\left(\mathbf{\Gamma}\right)$ and $B\left(\mathbf{\Gamma}\right)$ separated by a time interval t[26], and Equation (19) becomes:

$$\left\langle A(S^{z+t}\mathbf{\Gamma})B(S^{z}\mathbf{\Gamma})\right\rangle_{eq}=\left\langle A(S^{t}\mathbf{\Gamma})B(\mathbf{\Gamma})\right\rangle_{eq}-\beta VF_{e}\int_{0}^{z}\left\langle J\left(\mathbf{\Gamma}\right)\Delta A(S^{u+t}\mathbf{\Gamma})B(S^{u}\mathbf{\Gamma})\right\rangle_{eq}du \tag{20}$$

Then[26],

$$\left\langle A(S^{z-t}\mathbf{\Gamma})B(S^{z}\mathbf{\Gamma})\right\rangle_{eq}-p_{AB}\left\langle A(S^{z+t}\mathbf{\Gamma})B(S^{z}\mathbf{\Gamma})\right\rangle_{eq}=p_{AB}\beta VF_{e}\int_{-z}^{z}\left\langle J\left(\mathbf{\Gamma}\right)A(S^{u-t}\mathbf{\Gamma})B(S^{u}\mathbf{\Gamma})\right\rangle_{eq}du \tag{21}$$

where for A,B given by equations (13-14), $p_{AB}=1$, as discussed above. This is a transient response expression. However, if the system reaches a steady state, it will become independent of z, and give the limiting steady state expression $\langle A(S^{-t}\mathbf{\Gamma})B(\mathbf{\Gamma})\rangle_{F_{e}}=\lim_{z\to\infty}\langle A(S^{z-t}\mathbf{\Gamma})B(S^{z}\mathbf{\Gamma})\rangle_{eq}$, cf. Eq.(3.57) in[18] and Appendix B. The above requires the integrals of the correlation functions to exist, hence the correlations to decay faster than $1/t$. This relation, for $t\in[-\tau,+\tau]$, assumes a particular significance if applied to the functions $A\left(\mathbf{\Gamma}\right)$ and $B\left(\mathbf{\Gamma}\right)$ of Equations 13 and 15, in that the left hand side of Equation 21 is related to the measure of asymmetry $\langle\delta_{t}\rangle$ through Eqs.(17,18). It is this steady state result that we are interested in:

$$\langle\delta_{t}\rangle=\lim_{z\to\infty}\frac{\langle A(S^{z-t}\mathbf{\Gamma})B(S^{z}\mathbf{\Gamma})\rangle-\langle A(S^{z+t}\mathbf{\Gamma})B(S^{z}\mathbf{\Gamma})\rangle}{\langle|B(S^{z}\mathbf{\Gamma})|\rangle} \tag{22}$$

We will verify this relationship in numerical simulations in the next Section.

Note that if the function $B(\mathbf{\Gamma})=1$ for all $\mathbf{\Gamma}$, then clearly the right hand side of (22) would be zero in the steady state. If asymmetry is present, it therefore must result from the conditional average

through our choice of $B(\mathbf{\Gamma})$. This result might seem surprising on initial consideration, however the condition that we choose serves to align the peaks: the average of a sawtooth wave will be a constant (and therefore symmetric) if the phase of the wave is allowed to vary, but it will very asymmetric if the peaks are aligned (or the phase is fixed).

Now that we have expressed the asymmetry coefficient in terms of equilibrium ensemble averages and the TTCF, we consider its properties again. We note from above, that the expression (21) with $p_{AB} = 1$ applies to all phase variables A , irrespective of their parity under time reversal. First of all we observe that (21) shows that at equilibrium ($F_e = 0$), the asymmetry coefficient is zero. Although this is not a new observation, given (21) it becomes obvious. Similar considerations to those in Section 3.1 show that the asymmetry varies as F_e to leading order when $p_{A,F_e} = -1$ and as F_e^2 when $p_{A,F_e} = 1$. In addition we trivially observe that if $p_{AB} = 1$, the left hand side of (21) is zero, but note that this is also evident from consideration of the right hand side of that equation. In that case, the argument of the time-integral is an odd function and the time integral is from $-z$ to z, which will produce a value of *zero* for all z. The emergence of asymmetry can then be seen to come from the disturbance of integrand when $t \neq 0$ (*i.e.*a non-zero value of t results in a shift in the time at which values of A are determined and those at which the values of B are determined), which will clearly result in the argument no longer being an odd function, and therefore the integral will no longer be zero. This will be true in general, but in the special case that z is large, correlations decay and $A = B$ or $\dot{A} = B$, etc, the integral can be reformulated giving the expected result of zero. We point out that this is consistent with the argument of Giberti et al.[10] who argue that lack of interactions and therefore correlations will lead to temporally symmetric fluctuations.

4 Numerical results

Molecular dynamics simulations of color diffusion have been carried out in 2 Cartesian dimensions with a primitive cell containing 8 particles with kinetic temperature fixed at 1, a number density of $n = 0.4$ and timestep of 10^{-3}. The equations of motion interaction potential and relationship between the color current and dissipative flux are given in Section 2.1. We consider an equilibrium system as well as a range of nonequilibrium systems ($F_c = 0.5, 1, 1.5, 2, 3, 4$) , extending from the linear regime to the nonlinear regime and examine the FPs of J_c. Sets of ten independent simulations of least 3×10^6 timesteps were carried out for each value of color field, in order to determine the mean and the standard deviations of J_c, so to set the thresholds. These means and standard deviations of J_c and pressure are reported in Table 2.

Insert Table 2 near here

From the data we can see that the linear regime extends to approximately $F_c = 1.5$. For large J_c, large fluctuations (several standard deviations from the mean) are biased above the mean in the nonequilibrium systems; the same does not happen for the values of J_c at equilibrium, since they are symmetrically distributed around their mean of zero. The bias in the mean and deviations from the mean can be understood by considering the microscopic expressions for the properties considered. On the basis of these data, sets of 45 steady state simulations of 3.5×10^7 timesteps were carried out for each field. The average the FP of J_c with a threshold equal to $\mu + 2.5\sigma$ was evaluated for $\tau = 1$ and are shown in Figure 3A. Figure 3B shows the values of $\langle \delta_t \rangle$ for the FPs. All values are plotted with error bars being the standard error of the mean. The average FPs are obtained as averages of these runs and so are the $\langle \delta_t \rangle$'s. These values are also plotted with error bars.

Insert Figure 3 near here

Importantly, for $F_c = 0$, the value of $\langle \delta_t \rangle$ is zero to within numerical error at all times. This is an independent check of the accuracy of our results. Furthermore, at all other F_c, asymmetry is evident: we can see that the $\langle \delta_t \rangle$ initially increases; it reaches a maximum and starts decreasing. This behavior was also observed in our previous work[7,8]. From the definition of $\langle \delta_t \rangle$, it is obvious that this quantity vanishes at $t = 0$. As t increases, $\langle \delta_t \rangle$ departs from zero indicating asymmetry out of equilibrium, and showing that the approach to the peak of the FP is less steep than the departure from it. At a certain time $t > 0$, $\langle \delta_t \rangle$ starts to decrease due to the decay of the correlations, in the same way as previously described for a general odd function. All the previous results confirm the observations we made for different definitions of FP in our previous papers[7,8], attesting once more the presence of asymmetry of fluctuations, and the independence of this result on the definition of the FP.

The symmetries of various correlation functions were also considered. Sets of 65 independent simulations of 5×10^5 timesteps were carried out for $(F_c = 0.5, 1, 1.5, 2, 3, 4)$ in order to compute examples of correlation functions $\langle A\left(S^t\Gamma\right) B\left(\Gamma\right)\rangle$. The presence of asymmetry in t is expected for a generic odd property, such as the correlation between the flux J_c and the pressure P, as discussed above. Figure 4A displays the cross correlation $\langle J_c\left(S^t\Gamma\right) P\left(\Gamma\right)\rangle$ as a function of t for our system undergoing color diffusion with $F_c = 2$. The results are obtained as time averages from steady state runs and are the average values obtained from 65 runs of 5×10^5 timesteps with error bars.

Insert Figure 4 near here

We verify that for this function the time dependence of the correlation function fulfils the relevant properties of Table 1. At equilibrium, $\langle J_c(\Gamma) P(\Gamma)\rangle_{eq} = 0$, whereas it has a finite positive value when $F_c \neq 0$. We observe that for all fields, in the limits $t \to +\infty$ and $t \to -\infty$ the correlation functions

are equal, and equal to $\langle J_c \rangle \langle P \rangle$, as expected for this chaotic dynamics where correlations decay. We also note that at $t = 0$ the slope is different from zero, and that the value at $t = 0$ is different from that at large values of $\pm t$. This is consistent with the analysis at the end of Section 3.1. If, in the nonequilibrium system, the correlation has a value $\langle J_c(\Gamma) P(\Gamma) \rangle$ at $t = 0$, with slope different from zero, to then relax in both directions to $\langle J_c(\Gamma) P(\Gamma) \rangle \neq \langle J_c(\Gamma) \rangle \langle P(\Gamma) \rangle \neq 0$, for intermediate $|t|$, our cross correlation $\langle J_c(S^t\Gamma) P(\Gamma) \rangle$ must be different from $\langle J_c(S^{-t}\Gamma) P(\Gamma) \rangle$. For even functions, the presence of asymmetry can be measured by calculating $X_t(A,B) = C(z,t) - C(z,-t)$. For odd functions, due to their non-zero time-derivative at $t = 0$, we consider the departure of the profile from an anti-symmetric one by evaluating $X_t^{ODD}(A,B) = C(z,t) + C(z,-t) - 2C(z,0)$. By definition the value of X_t^{ODD} is 0 at $t = 0$. We can see from Figure 4B how the non-zero derivative and asymptotic values indicate the presence of a departure from an anti-symmetric behavior, which is the general situation out of equilibrium. There are choices of particular functions, such as the correlation of a function with itself or with its derivative, for which it can be proven and shown by numerical results, that no asymmetry is present. Figure 5A shows the color current autocorrelation $\langle J_c(S^t\Gamma) J_c(\Gamma) \rangle$ with $F_c = 2$, and in figure 5B the correlation between the color current and its derivative $\left\langle J_c(S^t\Gamma) \dot{J}_c(\Gamma) \right\rangle$ is shown for $F_c = 2$. In the first case the profile is perfectly symmetric within numerical error, as we can see from Figure 5C and in the second case the profile is perfectly anti-symmetric, and this is also shown in Figure 5C where $X_t^{ODD}\left(J_c, \dot{J}_c\right)$ is zero at all t. In contrast, the cross correlation $\langle J_c(S^t\Gamma) P(\Gamma) \rangle$ is asymmetric, as confirmed by the numerical results for $\langle \delta_t \rangle$ in Figures 5C. Note the similarity of the behaviour of the FPs in Figure 3 and of the correlation function in Figure 5. This is a natural consequence of the fact that the system relaxes from a peculiar state to the steady state with time scales that are dictated by the decay of the correlations.

Insert Figure 5 near here

We now provide numerical results confirming the TTCF expression for the asymmetry (21), and thus confirming the relationship on which we based our main argument in Section 3.2, *i.e.*that asymmetry must exist in general for correlations functions, and for the FPs in particular. Referring to Equation (21), we see that if we make z sufficiently large that a steady state is reached, the right hand side of our equations give $\langle \delta_t \rangle$, through equation (22). We therefore ran a set of 35 simulations consisting each of 10^6 transients starting from equilibrium values and going forward and backwards in time for a period $z + t$, with $t \in [-\tau, +\tau]$, $\tau = 1$, and with $z = 3$ so as to be far enough from the equilibrium starting point to consider our system well into the steady state.[27] We then evaluated the right hand side of equation (21). The numerical error in evaluation of the left hand side of equation

(21) from the transients is extremely high[28], and therefore these results are not shown. Instead, the left hand side of the equation was evaluated from the steady state simulations. Figure 6 shows the right hand side of Equation 21, scaled to give $\langle \delta_t \rangle$ through equation (22), and evaluated from the transient runs is equal to that evaluated as steady state average, to within numerical errors. The agreement of Figures 3B and 6 within the limits of error confirms the link between the presence of asymmetry with TTCF theory for the FPs of a deterministic and reversible system.

Insert Figure 6 near here

Finally we consider the dependence of $\langle \delta_t \rangle$ as a function of the field F_c. We select an arbitrary time $t = 0.1$ close to the peaks of the plot of $\langle \delta_t \rangle$ versus time. Figure 7 shows $\langle \delta_t \rangle$, at $t = 0.1$, of the average fluctuation path of color flux J_c, with $T_{HR} = 2.5\sigma + \mu$, as a function of the color field F_c applied. We see that $\langle \delta_t \rangle$ grows with the field in the linear regime: there are two contributions to the growth of $\langle \delta_t \rangle$. Firstly there is a direct contribution which we would expect to be linear for the odd property J_c, if the value of the threshold was fixed; then there is a growth due to an increase in the threshold, since μ increases linearly with F_c.

Insert Figure 7 near here

Conclusions

The presence of temporal asymmetries has been confirmed in various nonequilibrium molecular dynamics simulations and adopting various methods to detect them. Unlike earlier studies on particles systems, the model used does not have complications such as time-varying boundary conditions. A new definition of FP is introduced that allows a more rigorous analysis of the emergence of their asymmetry with an application of a field. FPs have been expressed by means of correlation functions and TTCF theory: thus for the first time we have been able to theoretically justify the asymmetries that have been observed previously in deterministic, reversible systems. This has allowed us to show for the first time that temporal asymmetries are a common property of deterministic and reversible nonequilibrium systems.

Appendix A

In reference[18], it has been shown how to obtain the TTCF expression for some particular cases. Consideration of equation (7.29) of that reference provides us with a route to a more general expression:

$$\langle B(S^z\mathbf{\Gamma})\rangle_{eq} = \langle B(\mathbf{\Gamma})\rangle_{eq} + \int_0^z \langle B(S^u\mathbf{\Gamma})\Omega(\mathbf{\Gamma})\rangle_{eq} du \tag{23}$$

where

$$\Omega(\mathbf{\Gamma})f(\mathbf{\Gamma}) = -\frac{\partial}{\partial\mathbf{\Gamma}}\cdot(\dot{\mathbf{\Gamma}}f(\mathbf{\Gamma})) = -f(\mathbf{\Gamma})\frac{\partial}{\partial\mathbf{\Gamma}}\cdot\dot{\mathbf{\Gamma}} - \frac{df(\mathbf{\Gamma})}{dt} + \frac{\partial f(\mathbf{\Gamma})}{\partial t} \tag{24}$$

and Ω is the dissipation function that appears in the Evans-Searles fluctuation relation[21]. Although equilibrium ensemble averages are used in (23), the dynamics represented by S are the nonequilibrium dynamics. The distribution function that is used in the ensemble average in equation (23) and in the definition of (24) is the distribution function preserved by the field free dynamics, so $\partial f/\partial t = 0$.

Interestingly, the isokinetic canonical distribution function with $\beta = (k_BT)^{-1}$ and using $K_0 = (dN - d - 1)k_BT/2$ is not preserved when the usual (see Chapter 6 of[18]) color diffusion equations are employed, and terms of all order in N are considered. A more problematic, but similar, situation has been observed when μ-thermostats have been employed (for more details see reference[29]). In the case of color diffusion, the problem that occurs relates to the subtraction of the streaming velocity, $\mathbf{u}$. Unlike the approximate streaming velocity, the real streaming velocity is a constant and not dependent on Γ, so the distribution function could be determined as usual, giving an isokinetic equilibrium distribution function:

$$f_{EQ}(\mathbf{\Gamma}) = \frac{e^{-\beta H_0(\mathbf{\Gamma})}\delta(K(\mathbf{\Gamma}) - K_0)}{\int e^{-\beta H_0(\mathbf{\Gamma})}\delta(K(\mathbf{\Gamma}) - K_0)d\mathbf{\Gamma}} \tag{25}$$

where K_0 is the required kinetic energy and the internal energy is given by:

$$H_0(\mathbf{\Gamma}) = K(\mathbf{\Gamma}) + \Phi(\mathbf{q}) = \sum_i \frac{1}{2m_i}\left(\mathbf{p}_i - \mathbf{u}\right)^2 + \Phi(\mathbf{q}). \tag{26}$$

If $\mathbf{u}$ is not known a priori, it can be estimated as $1/N\sum_{i=1}^N c_i\mathbf{p}_i$ which fluctuates at equilibrium, even though its average is zero. This leads to a change in the phase space contraction rate that is $O_N(1)$ (order 1 in N) , and no longer preserves (25), even when H_0 is redefined to account for the altered streaming term. An equilibrium distribution can be defined, but it requires that the proportionality constant between K_0 and k_BT is different. To circumvent this problem in this paper (which does not aim to realistically model a physical problem) we simply set $\mathbf{u} = \mathbf{0}$, obtaining a distribution function (25) and thermostatting $\sum_i \frac{1}{2m_i}\mathbf{p}_i{}^2 = K_0 = (dN - d - 1)k_BT/2$. A better approach if a physical system was to be studied would be use an iterative method to determine the streaming velocity. In this Appendix we show that for this system $\Omega = -\beta JF_eV$, and hence equation (19) follows.

In this Appendix we consider general thermostatted equations of motion,

$$\dot{\mathbf{q}}_i = \frac{\mathbf{p}_i}{m} + C(\mathbf{\Gamma})F_e\hat{\mathbf{n}}_x \tag{27}$$

$$\dot{\mathbf{p}}_i = \mathbf{F}_i + D(\mathbf{\Gamma})F_e\hat{\mathbf{n}}_x - \zeta(\mathbf{p} - \mathbf{P}) \tag{28}$$

The distribution function (25) is conserved by the equilibrium equations of motion. That is

$$\frac{\partial}{\partial t} f_{EQ}\left(\mathbf{\Gamma}, t\right) = f_{EQ}(\mathbf{\Gamma}, t)\Lambda(\mathbf{\Gamma}) - \beta\dot{H}_0(\mathbf{\Gamma}) f_{EQ}\left(\mathbf{\Gamma}, t\right) \tag{29}$$

where the quantity $\Lambda(\mathbf{\Gamma}) = -\frac{\partial}{\partial \mathbf{\Gamma}} \cdot \dot{\mathbf{\Gamma}}$ is the phase space compression rate of the system. Using the equations of motion, we can write the phase space compression rate as:

$$\Lambda(\mathbf{\Gamma}) = (dN - d - 1)\zeta. \tag{30}$$

We also find,

$$\dot{H}_0 = -JF_eV - 2\zeta K_0 = -JF_eV - \zeta(dN - d - 1)k_BT \tag{31}$$

Clearly (29) is zero at equilibrium ($F_e = 0$).

We can now evaluate Ω using (24), that is,

$$\Omega(\mathbf{\Gamma}) = \Lambda(\mathbf{\Gamma}) + \beta\dot{H}_0(\mathbf{\Gamma}) = -\beta J(\mathbf{\Gamma})F_eV \tag{32}$$

Hence we obtain the nonlinear response given by equation (19).

Appendix B

The equality of Section 3.2,

$$\left\langle A(S^{-t}\mathbf{\Gamma})B(\mathbf{\Gamma})\right\rangle_{F_e} = \lim_{z\to\infty}\left\langle A(S^{z-t}\mathbf{\Gamma})B(S^z\mathbf{\Gamma})\right\rangle_{eq}, \tag{33}$$

may be obtained from a transformation of coordinates as follows (c.f. Ref.[19]). Let $f_{F_e,z}$ be the probability density in phase space at time z, obtained with a field, F_e, and assume that the evolution is such that the probability distribution converges to a given stationary distribution. Then, the steady

state average obeys

$$\left\langle A(S^{-t}\mathbf{\Gamma})B(\mathbf{\Gamma})\right\rangle_{F_e} = \lim_{z\to\infty}\int A(S^{-t}\mathbf{\Gamma})B(\mathbf{\Gamma})f_{F_e,z}(\mathbf{\Gamma})\mathbf{d\Gamma} \tag{34}$$

while the probability density obeys $f_{F_e,z}(\mathbf{\Gamma}) = f_{F_e,0}(S^{-z}\mathbf{\Gamma})e^{-\int_{-z}^{0}\nabla\cdot\dot{\mathbf{\Gamma}}(S^s\mathbf{\Gamma})ds}$, as determined by the Liouville equation (cf. Eq.(32) in[19]). The coordinate transformation $\mathbf{X} = S^{-z}\mathbf{\Gamma}$ then yields

$$\left\langle A(S^{-t}\mathbf{\Gamma})B(\mathbf{\Gamma})\right\rangle_{F_e} = \lim_{z\to\infty}\int A(S^{z-t}\mathbf{X})B(S^z\mathbf{X})f_{F_e,0}(\mathbf{X})d\mathbf{X} = \lim_{z\to\infty}\left\langle A(S^{z-t}\mathbf{\Gamma})B(S^z\mathbf{\Gamma})\right\rangle_{eq} \tag{35}$$

since the Jacobian $|d\mathbf{\Gamma}/d\mathbf{X}|$ equals $e^{\int_0^z\nabla\cdot\dot{\mathbf{\Gamma}}(S^s\mathbf{X})ds}$, which is the inverse of the factor appearing in the evolved probability density, $f_{F_e,z}(\mathbf{\Gamma})$.

Acknowledgments

The authors wish to thank the Australian Research Council, The Queensland Parallel Computing Facility and the Australian National Facility for support of this work. We thank Peter J. Daivis, Stephen R. Williams and John F. Dobson for useful comments and Benjamin V. Cunning for discussions.

References

1. L. Bertini, A. De Sole, D. Gabrielli, G. Jona-Lasinio, and C. Landim, Phys. Rev. Lett., **87**, 040601 (2001).

2. L. Bertini, A. De Sole, D. Gabrielli, G. Jona-Lasinio, and C. Landim, J. Stat. Phys., **107**, 635 (2002).

3. L. Onsager and S. Machlup, Phys. Rev., **91**, 1505 (1953); S. Machlup and L. Onsager, Phys. Rev., **91**, 1512 (1953).

4. P. Gaspard, Ad. Chem. Phys., **135**, 83 (2007).

5. D. G. Luchinsky and P. V. E. McClintock, Nature, **389**, 463 (1997).

6. M. I. Dykman, P. V. E. McClintock, V. N. Smelyanski, N. D. Stein and N G Stocks, Phys. Rev. Lett. **68**, 2718 (1992).

7. C. Paneni, D. J. Searles, L. Rondoni, J. Chem. Phys. **124**, 114109 (2006).

8. C. Paneni, D. J. Searles, L. Rondoni, 2006 ICONN Proceedings Manuscript, IEEE Publication Co., Piscataway, U.S.A.

9. C. Giberti, L. Rondoni and C. Vernia, Physica A **365**, 229 (2006).

10. C. Giberti, L. Rondoni and C. Vernia, Physica D, **228**, 64 (2007).

11. H. B. G. Casimir, Rev. Mod. Phys. **17**, 343 (1945).

12. M. J. Klein, Phys. Rev. **97**, 1446 (1955).

13. H. Ichimura, Chin. J. Phys. **17**, 94 (1979).

14. D. Sánchez, M. Büttiker, Phys. Rev. Lett. **93**, 106802 (2004).

15. C. A. Marlow, R. P. Taylor, M. Fairbanks, I. Shorubalko, and H. Linke, Phys. Rev. Lett. **96**, 116801 (2006).

16. J. D. Weeks, D. Chandler and H. C. Andersen, J. Chem. Phys. **54**, 5237 (1971).

17. M. P. Allen and D. J. Tildesley, *Computer simulation of liquids*, Clarendon Press, Oxford (1987).

18. D. J. Evans and G. P. Morriss, *Statistical Mechanics of Nonequilibrium Liquids*, ANU E-Press, Canberra (2007).

19. D. J. Searles, L. Rondoni and D. J. Evans, J. Stat. Phys., **128**, 1337 (2007).

20. D. J. Evans, Physica A **118**, 51 (1983).

21. D.J. Evans and D.J. Searles, Ad. Phys. **51**, 1529 (2002).

22. G. M. Wang, E. M. Sevick, E. Mittag, D. J. Searles, and D. J. Evans, Phys. Rev. Lett., **89** , 050601 (2002).

23. This does not exclude that the previously introduced definitions of fluctuation paths may be cast in the present formalism.

24. There is no natural criterion to identify T_{HR}. However, the choice of T_{HR} and τ does not affect our theoretical treatment, hence in the numerical work we chose a value for T_{HR} that allows us to sample large fluctuations and also gather sufficiently good statistics. We typically choose a value of τ that is equal to several Maxwell times, after which no change in the form of the FP occurs.

25. D. A. McQuarrie, *Statistical Mechanics*, Harper and Row, New York (1976).

26. M.G. McPhie, P.J. Daivis, I.K. Snook, J. Ennis, and D.J. Evans, Physica A, **299**, 412 (2001).

27. Because of the Lyapunov instability and of the finite precision of numerical simulations, it was not possible, in practice, to run the transients backwards for more than a time of about 1. Therefore we exploited the time reversal properties of the system in order to calculate the values assumed by our function for negative times, directly from the values obtained in the forward run.

28. The probability of finding a peak exactly at time z of the transient is very low (at high fields it is much lower than in the corresponding steady state because much of the trajectory is in a state close to the initial equilibrium state where large deviations are even more unlikely to be observed). An enormous number of cycles should be run in order to obtain data with reasonable statistics, and while the data we were able to obtain was in agreement with the results, the statistical error was so large that the values were not very meaningful.

29. J.N. Bright, D.J. Evans and D.J. Searles, J. Chem. Phys, **122**, 194106, (2005).

Figure Captions

Figure 1: A sample of the time evolution of the dissipative flux, J, in a fluid subject to a field, F_e. The way in which fluctuation paths are selected is shown: troughs are converted to peaks and the average FP ($\langle Y(t) \rangle$) is constructed as average of such peaks centered in t_{STAT}.

Figure 2: A schematic illustration of the existence of asymmetry in systems where correlations decay and $\frac{d^n C(z,t)}{dt^n}|_{z,t=0} \neq 0$, for any of $n = 1, 3, 5, ...$

Figure 3: A: Average fluctuation path (FP) of the color current from the average of 45 steady state runs with error bars (equal to the standard deviation of the mean). B: $\langle \delta_t \rangle$ for the average fluctuation path of the color current from the averages of 45 runs with error bars (equal to the standard error of the mean).

Figure 4: A: Cross correlation function of color current J_c and pressure P from the average of 65 steady state runs with error bars (equal to the standard error of the mean) and with color field $F_c = 2$. B: Coefficient of asymmetry X_t^{ODD} , for $F_c = 2$, with departure from zero indicating asymmetry out of equilibrium.

Figure 5: A: Autocorrelation function of color current J_c from the average of 65 steady state runs with error bars (equal to the standard error of the mean) and with color field $F_c = 2$. B: Correlation function of color current J_c with its derivative from the average of 65 steady state runs with error bars (equal to the standard error of the mean) and with color field $F_c = 2$. C: The value of X_t which measures the departure of the cross-correlation function $\langle J_c(S^t\Gamma)J_c(\Gamma)\rangle$ from symmetric behavior, and values of X_t^{ODD} which measures the departures from anti-symmetric behavior of $\langle J_c(S^t\Gamma)\dot{J}_c(\Gamma)\rangle$ and $\langle J_c(S^t\Gamma)P(\Gamma)\rangle$. All data are computed as average of 65 runs with error bars (equal to the standard error of the mean) with color field $F_c = 2$.

Figure 6: The values of $\langle \delta_t \rangle$ for the average fluctuation path of the color current from averages of 35 transient runs with error bars (equal to the standard error of the mean), calculated using the right hand side of equation (21) with $z = 3$. This can be compared to the results obtained using a steady state expression as shown in Figure 3b.

Figure 7: $\langle \delta_t \rangle$ as a function of the field F_c at arbitrary time $t = 0.1$ close to the peaks of the δ_t,with $T_{HR} = 2.5\sigma + \mu$.

Table 1: Properties of correlation functions, $C(z,t) = \langle A(z)B(z+t)\rangle$ obtained by considering the symmetry of the functions on time-reversal and change of the sign of the field, and assuming that correlations decay in the all the systems.

Ensemble/Dynamics	**Condition**	$\mathbf{C(z,t)}$	$\mathbf{\lvert C(z,t) - C(z,-t)\rvert}$	$\mathbf{\lim_{t\to\infty} C(z,t)}$	$\mathbf{\lim_{t\to\infty}(C(z,t) - C(z,-t))}$ [a]
equilibrium	no special condition	$\langle A(z)B(z+t)\rangle_{eq}$	0	0	0
equilibrium	$p_{AB} = -1$	0 when $t = 0$	0	$\langle A\rangle_{eq}\langle B\rangle_{eq}$	0
steady state	$A = B$	$\langle A(z)A(z+t)\rangle$	0	$\langle A\rangle^2$	0
steady state	$A = \dot{B}$ or $B = \dot{A}$	$\langle A(z)\dot{A}(z+t)\rangle$	0	0	0
steady state	$C(z,t)$ even funct. of F_c; linear regime	$\langle A(t)B(z+t)\rangle_{eq}$	0	$\langle A\rangle_{eq}\langle B\rangle_{eq}$	0
steady state	no special condition	[b]	[b]	$\langle A\rangle\langle B\rangle$	0
transient response: z=0; equilibrium at $z = 0$	$p_A = -1$	[b]	[b]	0	0
transient response: z=0; equilibrium at $z = 0$	$p_{AB} = -1$	0 when $t = 0$	[b]	[b]	0

[a] This is expected to be non-zero, in general. For example in a transient experiment where an equilibrium ensemble average is carried out, but $t \neq 0$ and $z \neq 0$.

[b] These values are expected to be non-zero, in general.

Table 2: Mean μ and standard deviation σ of color current J_c as averages from 10 runs with corresponding standard errors(three times the standard deviation of the means out of the runs).

F_c	$\mu(J_c)$	$\sigma(J_c)$
0	0 ± 0.006	0.341 ± 0.005
0.5	0.021 ± 0.007	0.342 ± 0.004
1	0.043 ± 0.007	0.343 ± 0.005
1.5	0.069 ± 0.005	0.345 ± 0.003
2	0.101 ± 0.008	0.35 ± 0.003
3	0.196 ± 0.023	0.365 ± 0.006
4	0.341 ± 0.019	0.38 ± 0.007

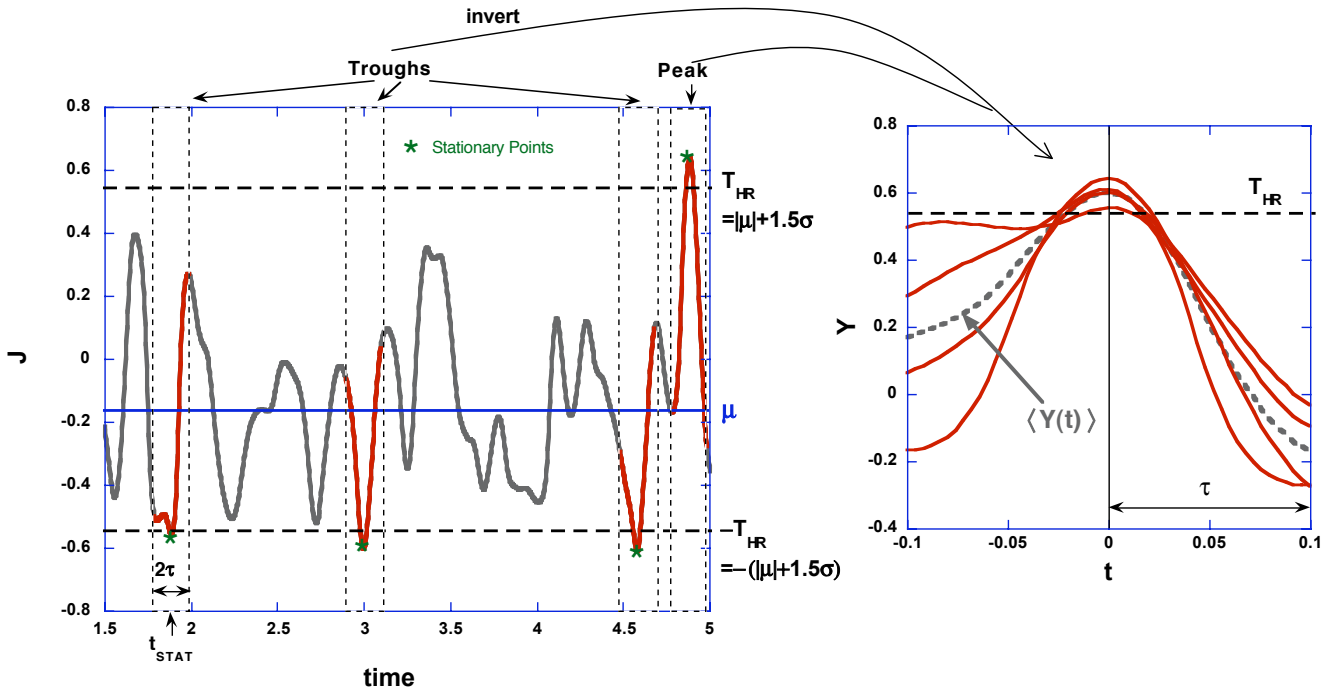

Figure 1. Paneni, Searles, Rondoni

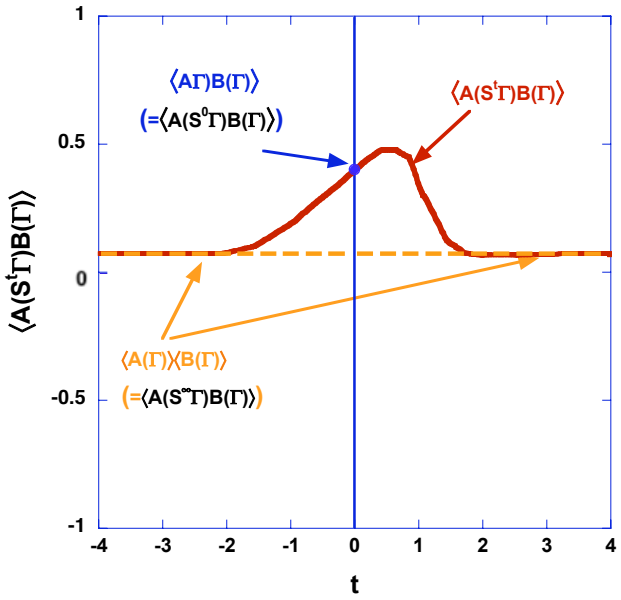

Figure 2. Paneni, Searles, Rondoni

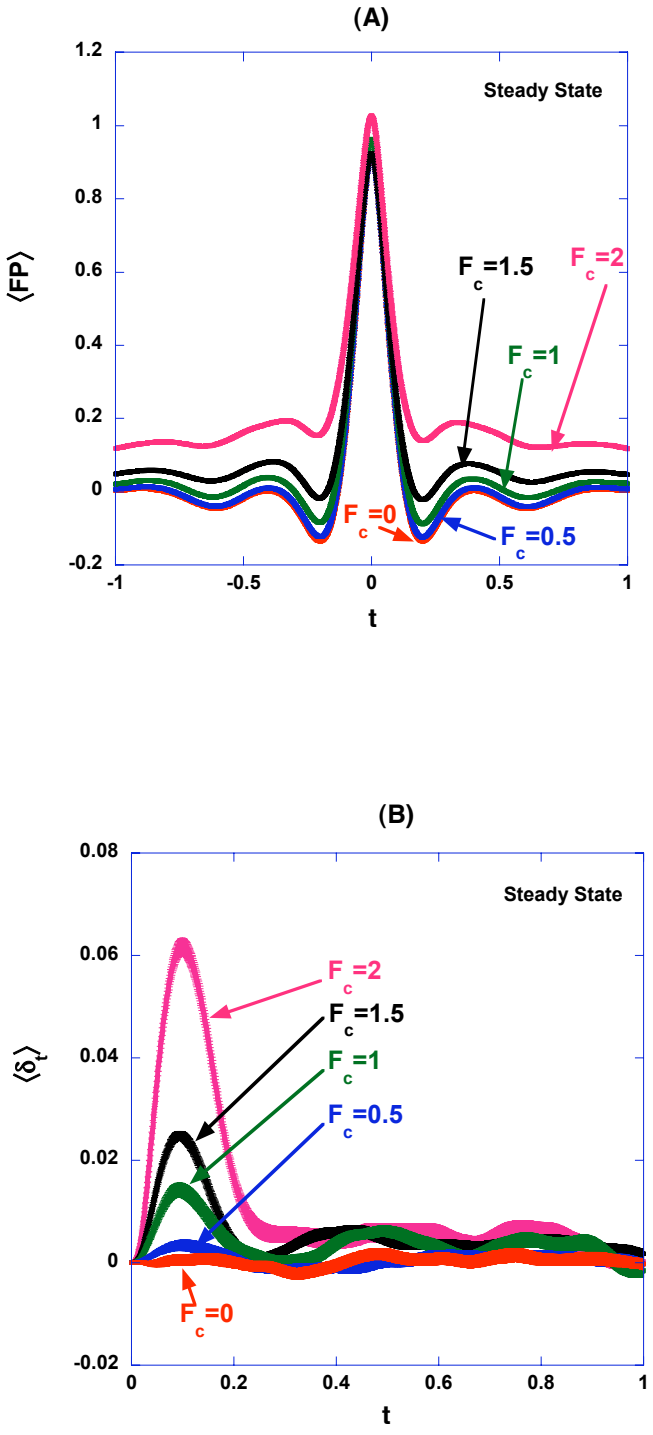

Figure 3. Paneni, Searles, Rondoni

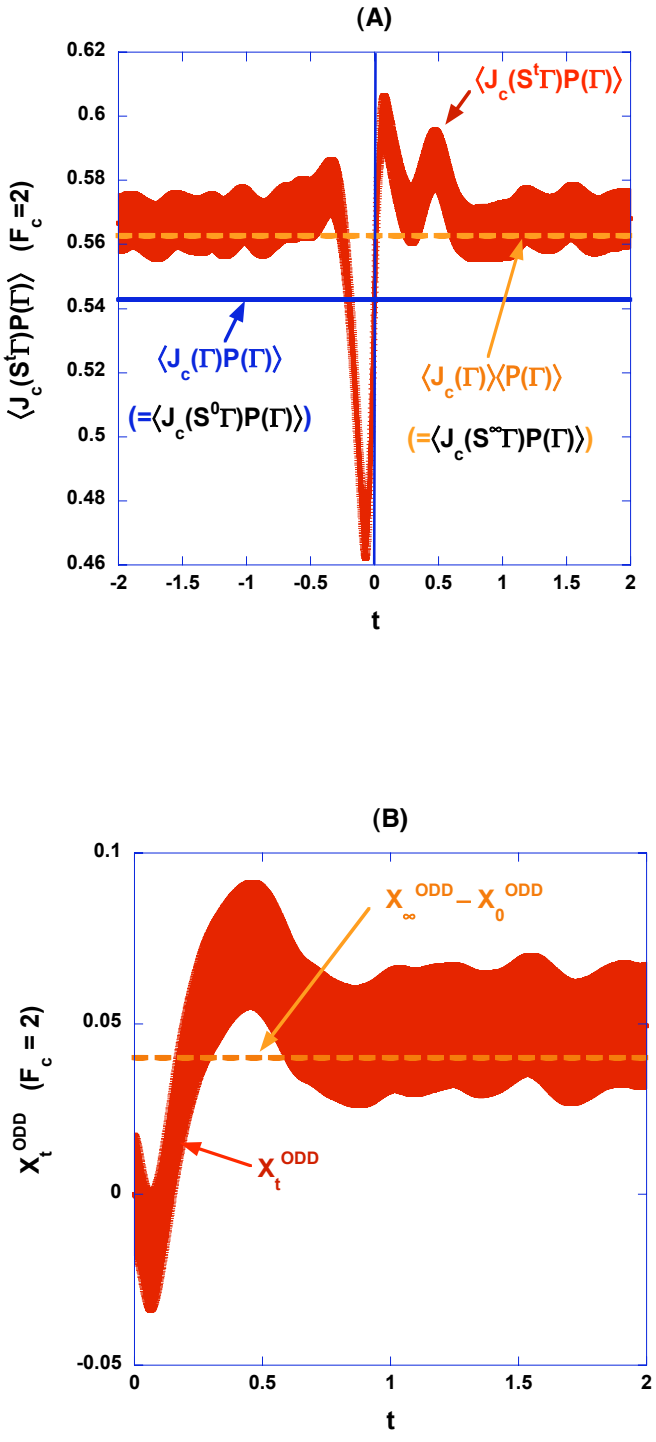

Figure 4. Paneni, Searles, Rondoni

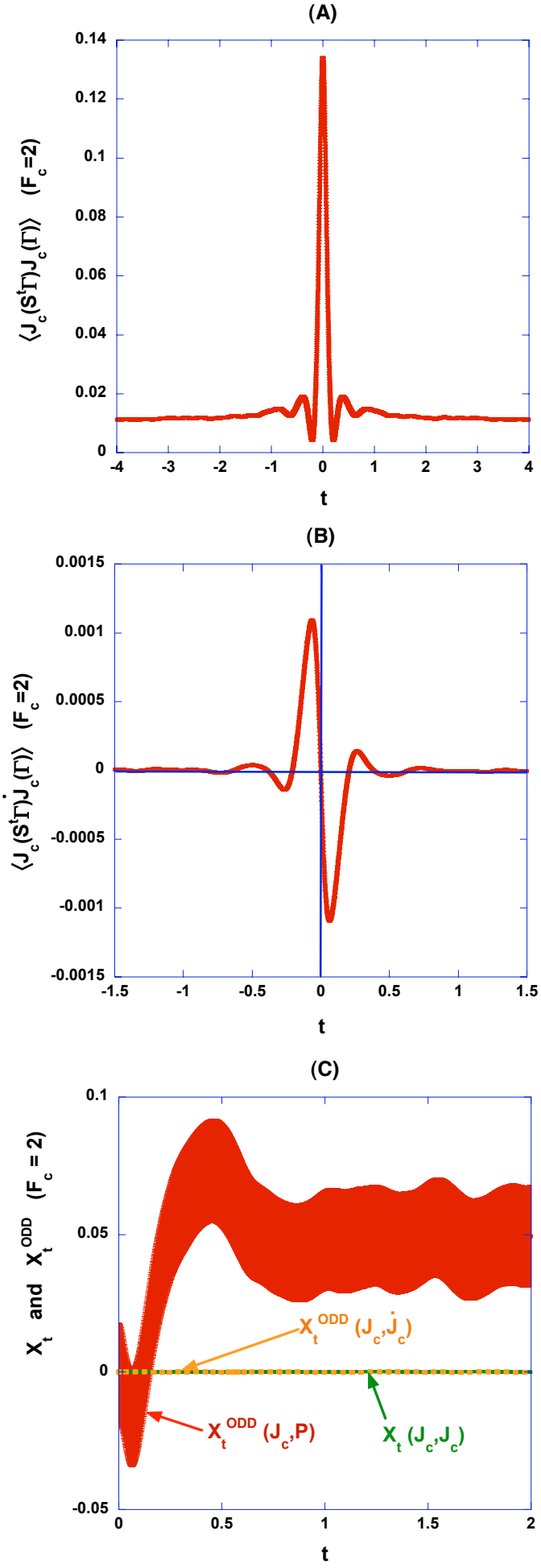

Figure 5. Paneni, Searles, Rondoni

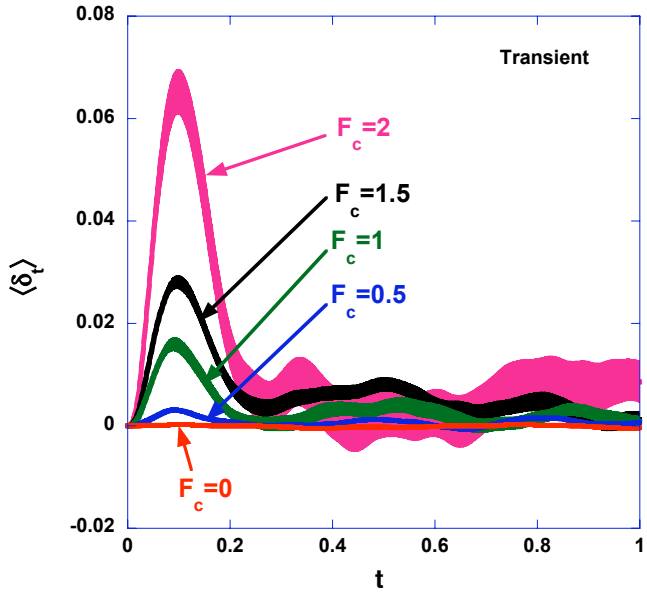

Figure 6. Paneni, Searles, Rondoni

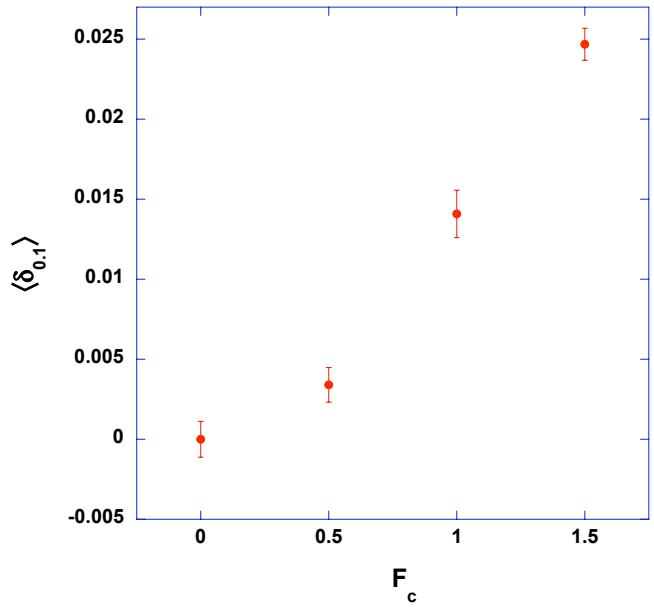

Figure 7. Paneni, Searles, Rondoni